

Design and Construction of Large Size Micromegas Chambers for the Upgrade of the ATLAS Muon Spectrometer

Philipp Lösel and Ralph Müller, *on behalf of the ATLAS Muon Collaboration*

Abstract—Large area Micromegas detectors will be employed for the first time in high-energy physics experiments. A total surface of about 150 m^2 of the forward regions of the Muon Spectrometer of the ATLAS detector at LHC will be equipped with 8-layer Micromegas modules. Each layer covers more than 2 m^2 for a total active area of 1200 m^2 . Together with the small strip Thin Gap Chambers they will compose the two New Small Wheels, which will replace the innermost stations of the ATLAS endcap muon tracking system in the 2018/19 shutdown.

In order to achieve a 15% transverse momentum resolution for 1 TeV muons, in addition to an excellent intrinsic resolution, the mechanical precision of each plane of the assembled module must be as good as $30 \text{ }\mu\text{m}$ along the precision coordinate and $80 \text{ }\mu\text{m}$ perpendicular to the chamber.

The design and construction procedure of the Micromegas modules will be presented, as well as the design for the assembly of modules onto the New Small Wheel. Emphasis will be on the methods developed to achieve the challenging mechanical precision.

Measurements and simulations of deformations created on chamber prototypes as a function of thermal gradients, internal stress (mesh tension and module fixation on supports) and gas over-pressure were essential in the development of the final design.

During installation and operation all deformations and relative misalignments will be monitored by an optical alignment system and compensated in the tracking software.

I. INTRODUCTION

AFTER the long shut down 2 (2018/19) and the related upgrade of the Large Hadron Collider (LHC) at CERN the luminosity will reach values around $2 \cdot 10^{34} \text{ cm}^{-2} \text{ s}^{-1}$. The number of primary vertices per bunch crossing and the background rate will increase proportionally. As a consequence the background hit rate in the innermost endcap region of the muon spectrometer of the ATLAS detector [1] (Small Wheel) will reach values above 10 kHz cm^{-2} , whereas the currently installed precision tracking detectors will become ineffective at hit rates of $\approx 2 \text{ kHz cm}^{-2}$. For this reason the detectors in the inner endcap region will be replaced by large size Micromegas (MICRO MESHed Gaseous Structure [2]) and sTGC (small Thin Gap Chamber [3]) detectors. While the sTGC detectors will be used mainly for triggering, the Micromegas detectors are foreseen mainly as precision tracking chambers. For redundancy both detector types are

designed to take over the other task as well. In this case the goal of the Micromegas would be to provide information to the trigger system [4], whether the traversing muon originated at the interaction point or not. In the present setup of the ATLAS muon spectrometer only the middle part (Big Wheel) of the three endcap regions is read out on trigger level including interaction point tracking. Fig. 1 shows three possible track constellations which lead to an accepted muon track in this region.

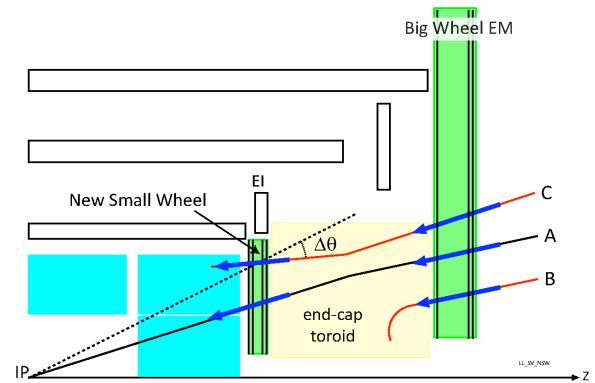


Fig. 1. Schematic drawing of a quarter of the ATLAS detector with possible tracks in the endcap region. Track A leaves a track in all detector regions and points towards the interaction point. Track B gives only a signal in the Big Wheel and Track C does not point towards the interaction point. Only Track A corresponds to an acceptable muon.

Combining the information of the Small Wheel and the Big Wheel a clear distinction between a muon coming from the interaction point and background hits will be possible. For this an angular resolution better than 1 mrad is necessary in the NSW.

Extrapolating the current trigger rate in the endcap, see fig. 2, to the luminosity after the second long shutdown indicates that the rate will be close to the bandwidth limit. The reason for this high trigger rate is caused by background events imitating the signals of true muons. Including the small wheel in the level one trigger, the total rate is expected to reduce by a factor of 5.

II. WORKING PRINCIPLE OF RESISTIVE STRIP MICROMEGAS DETECTORS

Micromegas detectors are high rate capable precision tracking devices. They consist of three planar structures: a copper cathode, a stainless steel micro mesh and anode strips on

Manuscript received August 12, 2015.

Ph. Lösel, Ludwig-Maximilians-Universität, Munich, Germany (telephone: +49 89 289 14160, e-mail: philipp.loesel@physik.uni-muenchen.de).

R. Müller, Ludwig-Maximilians-Universität, Munich, Germany (telephone: +49 89 289 14160, e-mail: ralph.mueller@physik.uni-muenchen.de).

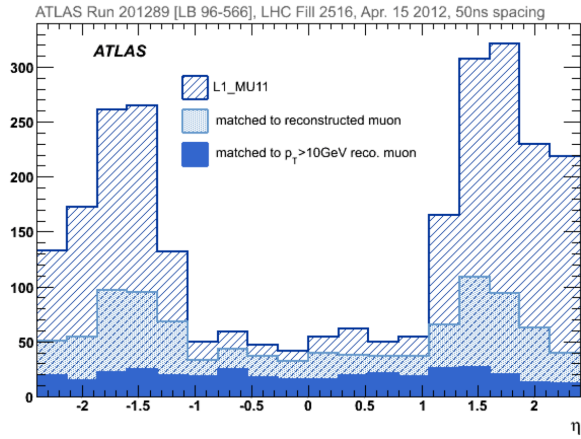


Fig. 2. Trigger rate in the ATLAS detector (April 2012) [5]. The rate in the endcap region ($|\eta| > 1$) is dominated by fake triggers. Counting only real muon events with $p_t > 1$ TeV, the trigger rate is flat in the whole detector (solid blue histogram).

printed circuit boards (PCBs). As shown in fig. 3 a traversing charged particle ionizes the gas along its path through the detector.

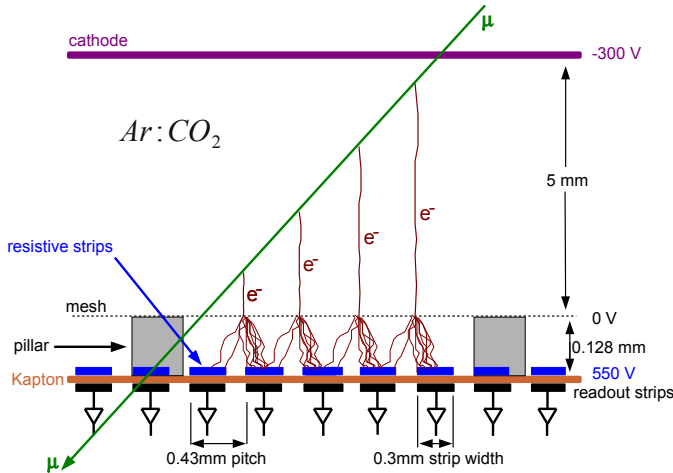


Fig. 3. Sketch of charged particle detection using a Micromegas detector. A muon (green) traverses the detector ionizing the $Ar:CO_2$ 93:7 gas. The electrons (red) drift to the mesh and cause avalanches between the mesh and the anode strips. The accumulated charge is coupled capacitively to the readout strips underneath the anode strips.

In the drift region the electron-ion pairs are separated due to the electrical field between the cathode and the mesh of around $E_{drift} \approx 600$ $V\,cm^{-1}$. The electrons drift towards the mesh and into the amplification region where an avalanche is forming by secondary ionisation in the narrow region between mesh and resistive strips of $d_{amp} = 128$ μm . Typical amplification fields are here $E_{amp} \approx 43$ $kV\,cm^{-1}$ leading to a gas gain of a few 1000. Discharges between mesh and strips can occur when the charge density in the high field in this region exceeds the Raether limit of 2×10^8 $e\,mm^{-2}$ [6], e.g. when a strongly ionizing ion enters a detector having been set up for detection of minimum ionizing muon. This is non-destructive but causes a temporarily reduced amplification field and thus deadtime. At standard micromegas the whole detector

gets insensitive until the field is re-established, as the potential between the anode and the mesh equilibrates. To prevent this global voltage drop a layer of resistive strips is added on top of the readout strips with a resistivity of ≈ 10 $M\Omega\,cm^{-1}$ [7]. The local discharge affects only one or a few strips and the high resistivity of the anode strips allows for an equilibration of the local potentials on a tiny region only and thus the fast breakdown of the discharge streamer and a fast recharge process of the anode. Only a negligible part of the detector is then affected by such a discharge. For electronic readout the charge collected on the resistive strips is capacitively coupled to the readout strips. They have a width of $= 300$ μm and a pitch of 425 μm or 450 μm depending on the module in the New Small Wheel. The homogenous tiny distance between anode and mesh is established by a regular structure of pillars made lithographically of Pyralux coverlay.

III. NEW SMALL WHEEL SECTOR DESIGN

The New Small Wheel (NSW) is designed to have the identical segmented structure like the current Small Wheel. It will be subdivided in eight alternating small and large sectors as shown in fig. 4.

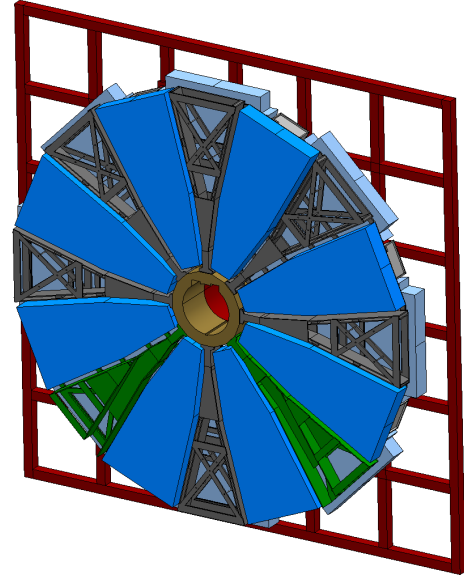


Fig. 4. The New Small Wheel with eight alternating small (dark blue) and large (light blue) sectors. To cover the whole region of the NSW the sectors overlap partially.

For the Micromegas each sector will be subdivided into two subsectors. There will be four trapezoidal types of Micromegas modules with different dimensions (see fig. 5), which are built and assembled in four different construction sites, see table I.

SM1	Italy
SM2	Germany
LM1	CERN, Greece and Russia
LM2	France

TABLE I
TABLE OF CONSTRUCTION SITES FOR THE FOUR MICROMEGAS MODULES OF THE NSW PROJECT. FOR DETAILS SEE TDR [5].

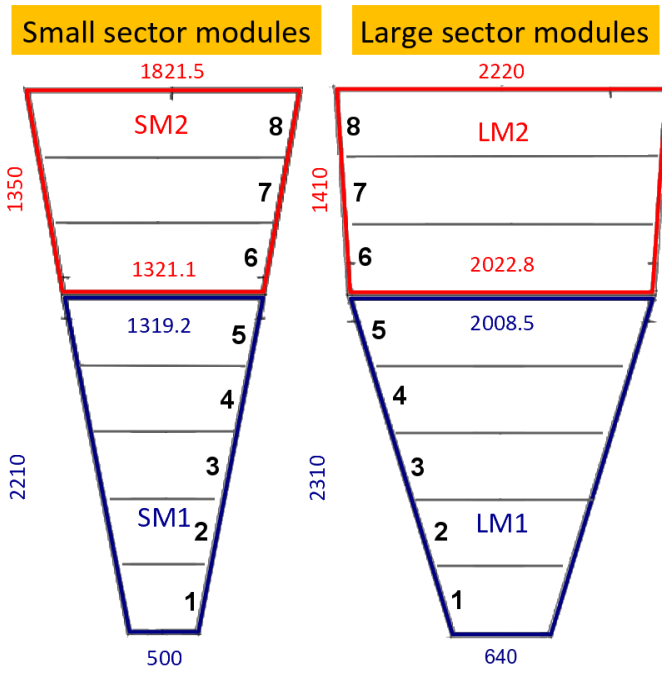


Fig. 5. Small and large sectors of the NSW divided into four trapezoidal modules with different dimensions. All units are in mm. For each sector the active readout plane is subdivided into eight readout PCBs and two detector modules.

To reach an optimal track resolution each module consists of eight consecutive Micromegas detectors, which are formed by two quadruplets (see fig. 13). Each quadruplet is constructed of five sandwich panels, see section IV and VI. Two layers of a quadruplet have a strip configuration parallel to the upper and lower bound, so called η -strips. The other two layers have stereo strips tilted by $+1.5^\circ$ (s -strips) and -1.5° (s' -strips) with respect to the η strips. The stereo strips deliver a rough information about the azimuthal φ -coordinate of the muon. Between the double quadruplet structure a spacer frame will be installed for stable mounting.

A Micromegas sector is sandwiched by sTGCs.

IV. PANEL CONSTRUCTION USING A STIFFBACK

In order to reach the desired position resolution of better than $100 \mu m$ in a single detector layer, the mechanical requirements of each panel are very strict. The panels, sandwiches of FR4 PCB sheets with an aluminum honeycomb core, need to have a surface planarity of better than $80 \mu m$. Even more strict is the requirement for readout-boards: the horizontal deviation of the readout strips position must not exceed $30 \mu m$ [5].

The four construction sites are using similar methods for the panel constructing to reach the mechanical requirements. Individual adaptations are accounted for by locally available infrastructure and manpower. The idea is to transfer the planarity of a very planar surface, e.g. a granite table, to PCBs by application of vacuum, see fig. 6. A frame of extruded aluminum bars and a honeycomb structure are glued on top of the PCB for stabilisation and reinforcement. A second PCB-layer, sucked down again to a planar surface,

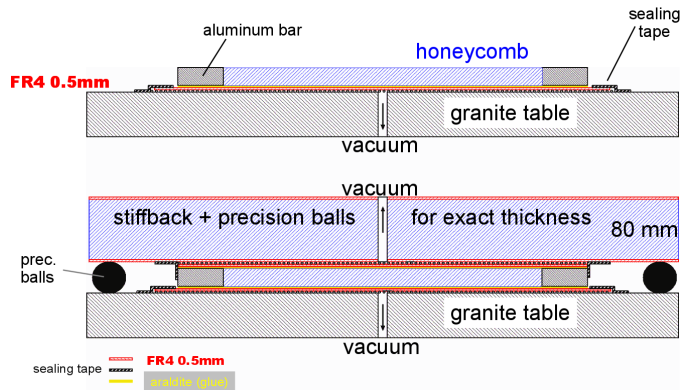


Fig. 6. The two steps of glueing a sandwich by use of a stiffback. The upper picture shows the final assembly of the first glueing step, the lower part the second step. The lower planar surface of the stiffback contains many small holes for vacuum suction. The honeycomb is microperforated and contains a few manually drilled channels. The distance between the stiffback and granite surface is controlled by exact distance pieces like the balls from ball bearings shown here.

is glued simultaneously or in a second step to this PCB-aluminum frame-honeycomb-structure.

Thus, two slightly different methods will be used to build the panels. In both ways at least one of the planar reference surfaces is a so called stiffback, a stable and accurate holding structure.

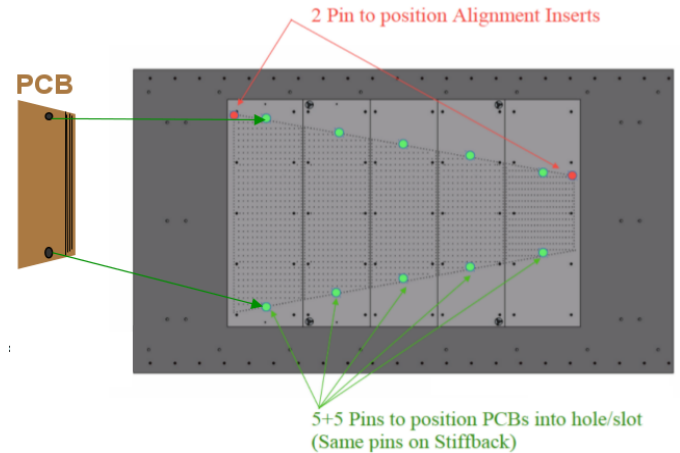


Fig. 7. Readout PCBs are positioned on reference surfaces (light gray) made of precision surface massive vacuum suction ground plates. The stiffback, not shown here, is constructed similarly. Both reference surfaces enable exact positioning of readout PCBs via alignment pins and mutual alignment by commercial tapered interlocks.

Stiffbacks will be either precision surface massive aluminum vacuum suction ground plates (see fig. 7) or relatively light sandwiches based on carbon fiber technology sheets or aluminum sheets, both with aluminum honeycomb core, built as a negative of a granite table. The choice of the material is driven partly by available infrastructure. A lightweight version of a stiffback consists of two 1mm thick aluminum plates sandwiching an 80 mm thick honeycomb core. For production an aluminum plate is sucked to a flat granite table and adopts its planar surface. Subsequently an 80 mm thick aluminum honeycomb is glued onto the plate to preserve the

flatness of the plate. Finally a frame with vacuum suction ports surrounding the honeycomb and a second plate will be glued on top. As glue the two component adhesive ARALDITE 2011 is used for the stiffback as well as later for the panels.

The honeycomb is micro perforated with additional channels drilled manually before glueing to allow for faster air exhaust. To use the stiffback as a vacuum suction surface many small holes are drilled into the planar surface of the stiffback for vacuum buildup between the reference surface and the PCB sheet to be attached.

The following explains both methods that will be used for panel glueing, the single step glueing procedure or the two-step process.

A. Two Step Glueing Technique

The method to build a panel is similar to the construction of the full aluminum stiffback. Here, each surface sheet of a panel will consist of three or five PCBs since single sheets in this size are not available (see fig. 5). Aluminum honeycomb is used as sandwich core. In the following we distinguish between drift- and readout-boards.

The production of drift-panels is less sophisticated. For the SM2 module all PCB-sheets forming a drift-plane will be positioned on the planar reference table by use of exact distance pieces aligned against an external frame. Sucking them down to the granite table fixes their position (see fig. 8). An aluminum frame of extruded aluminum bars is glued on top of the sheets. The aluminum frame has a height of 10 mm. For reinforcement a 10 mm thick aluminum honeycomb is glued inside this frame. This first step of the glueing process is indicated in the upper part of fig. 6.

After curing, the product of the first glueing step is removed from the granite table and sucked to a predefined position on the stiffback. The sheets for the second side of the panel are positioned on the planar reference table. Finally the stiffback is turned upside down and the product of the first glueing step is glued to these PCB sheets. The relative position of both planes is hereby referenced again by exact distance pieces aligned to the external frame.

Precision distance pieces, balls in fig. 6, between the granite table and the stiffback ensure the correct thickness and parallelism of the panel. The lower part of fig. 6 shows the setup during curing of the second step.

B. Single Step Glueing Technique

In the single step glueing technique two stiffbacks with pins for mutual alignment and further pins for exact positioning of PCB sheets are used instead of the granite table-stiffback combination. A photograph of the construction of a prototype can be seen in fig. 9.

One set of PCB sheets each is sucked against the surface of the respective stiffback. The aluminum frame and the honeycomb are then glued in a single step in between.

C. Precise Alignment of the Readout Strips for the Glueing Process

During production of readout sandwich-panels the challenging requirement of the exact positioning of the readout-strips

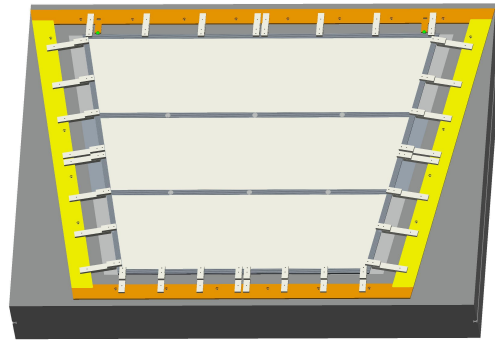


Fig. 8. The external reference frame for module SM2 on the granite table. Exact distance fingers allow for the positioning of the drift PCBs, of the extruded aluminum frames and for the alignment of the upper and lower PCB plane when the stiffback is used.

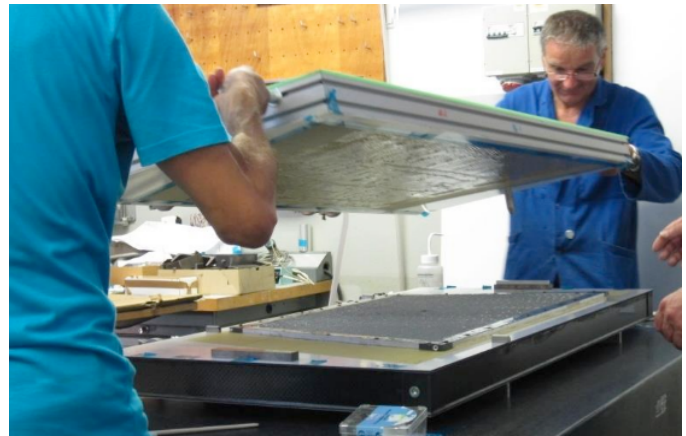


Fig. 9. Glueing of a prototype panel in a single step process using the double stiffback method. Two sets of PCB sheets will be sucked to the respective stiffback surface using small holes in the surface sheets of the stiffback. The honeycomb and aluminum bars are then glued in between.

must be met and each sheet must be precisely aligned within 30 μm to a global reference before sucking it to the granite table.

On each readout PCB two precise markers are produced in the same lithographic process as the readout strips. These markers are positioned left and right of the readout strips. Their position is very accurately defined in regard to the position of the readout strips. The markers are positioned vertically in the middle of the PCB.

For the single step glueing process precise alignment structures, a hole and an elongated hole to allow for thermal expansion, will be drilled into the PCBs at the position of the markers. The stiffbacks in fig. 9 contain matching alignment pins.

For the two step glueing process a precise washer containing a hole and a second one containing an elongated hole will be glued with very high precision and optically controlled on top of the markers. For the SM2 module an alignment frame with

six alignment pins is used to position the PCBs by means of the washers on the granite table. As global reference serve two 16 mm diameter pins. These are permanently installed on the granite table. A V-shaped and line-shaped contact piece provide the correct position of the alignment frame against these external references. For details see fig. 10. The relative position of V-shaped and line-shaped contact pieces against the six alignment pins is done in a single milling step and will be controlled on a precise coordinate measurement machine.

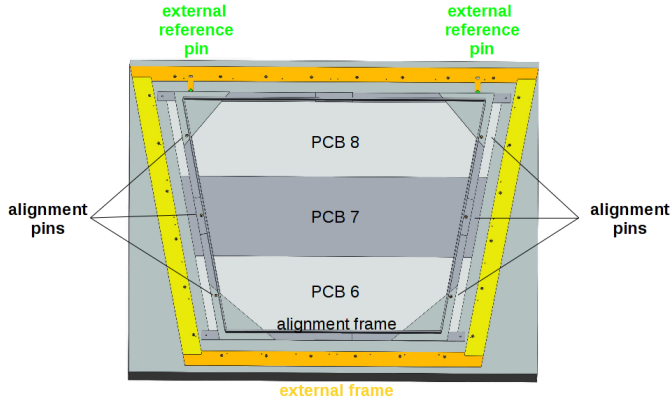


Fig. 10. The alignment frame for the SM2 module. Two precision pins (green) define the position of the readout panels on the granite table. They are mounted on an external permanently installed reference frame. The alignment frame attaches both pins by a V-shaped and a line-shaped contact piece respectively. Six 8 mm precision pins provide guidance for the three readout PCBs of the SM2 module. The pins fit exactly into precision washers, a round one and an elongated one on opposing sides of the PCBs, that are glued concentrically on top of precision markers. These markers are produced in the same lithographic step as the readout strips and reference with high accuracy the position of the strips. A relative alignment of the PCBs with an accuracy better than $30 \mu\text{m}$ is expected.

The remaining glueing process is similar to the production of the drift panels.

V. TREATMENT OF THE MICROMESH

For the NSW detectors a stainless steel micromesh with a wire diameter of $28 \mu\text{m}$ and a distance between the wires of $50 \mu\text{m}$ is foreseen. It will be mounted on the mesh frame of the drift panels. Precise 5.06 mm thick extruded bars provide the correct distance between mesh and the cathode surface. The mesh will thus be attached to ground potential. This so called floating mesh construction has the advantage that the amplification regions are still accessible even after the mounting of the meshes, an important feature for these large area detectors. Before glueing the meshes all drift panels must be leak tested and all meshes and panels must be dust and dirt free.

The meshes will be stretched with a homogeneous tension of 10 N cm^{-1} using pneumatic clamps, as shown in fig. 11, and glued to transfer frames. This process can be centralized and decoupled from the production sites for drift panels. The meshes will be transferred and glued in a later step to the mesh frame of a drift panel. The mesh frame consists of extruded aluminum bars with enlarged surface optimized for glueing, see fig. 12.

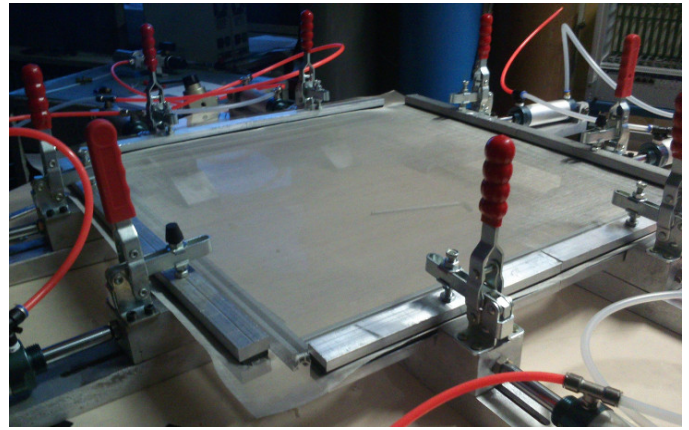


Fig. 11. Prototype setup for stainless steel mesh stretching. A $60 \times 60 \text{ cm}^2$ mesh is stretched using eight pneumatic clamps. For the final mesh size of the SM2 module 24 pneumatic clamps will be needed.

The extruded bars are screwed and glued to the cathode sides of the drift panels. The additional glueing provides gas tightness between the active detector volume and the honeycomb volume. The mesh is then glued to the mesh frame and the transfer frame can be reused after cleaning for the next mesh.

For the gas tightness an O-ring will be used in the groove between the mesh frame and the outer drift frame. The latter defines the distance between anode and cathode and thus the drift region. The upper right corner of a SM2 frame is shown in fig. 12.

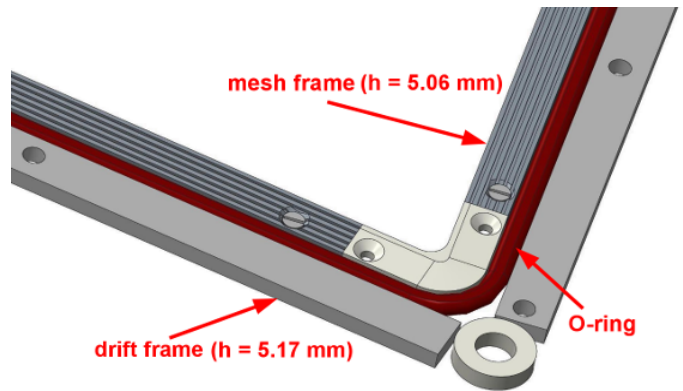


Fig. 12. Detail of the mesh frame, which will be screwed and glued on a drift panel. The mesh will be glued on top of the mesh frame. An O-ring between mesh and drift frame will ensure gas tightness.

VI. VERTICAL QUADRUPLLET ASSEMBLY IN A CLEAN ROOM

Fig. 13 shows a schematic cross section of a quadruplet.

During the assembly of the five panels it is important that all layers are mounted parallel and that all strips in all four readout layers follow with highest accuracy their theoretical coordinates. This means that the two readout panels need to be precisely aligned. Figure 14 shows the method to achieve this using two precise alignment pins mounted to one of the readout panels and a round and an elongated precision insert

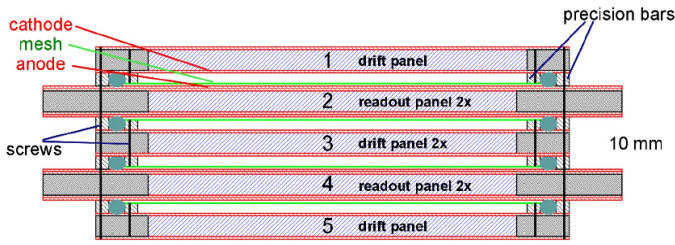


Fig. 13. Scheme of the five sandwich panels assembled to a quadruplet. The four active gas volumes between the drift and readout panels are defined by extruded precision drift bars. Similarly, extruded mesh bars define the exact distance of the micromeshes from the cathodes. In this design the meshes can be removed from the anode structures. Electrically they will be coupled to ground potential.

in the second readout panel. The precision pins and inserts must have a relative clearance of $25 \mu\text{m}$ at the maximum.

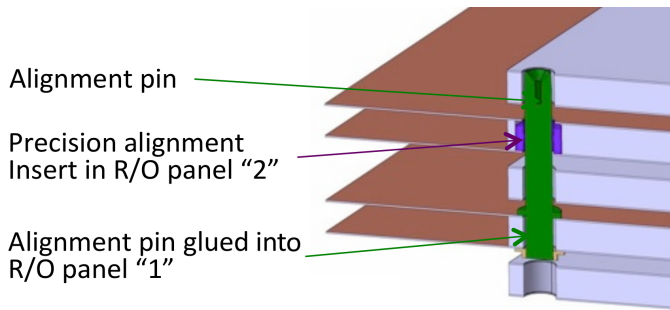


Fig. 14. Precision pins are used for the alignment of the readout panels. Two precision pins are glued to the lower readout panel. The upper readout panel has two precision inserts, a round one and an elongated one, to ensure the alignment between the readout panels.

In addition to a precise diameter the pin also needs to be exactly perpendicular to the readout panel. In fig 15 a tool for the correct pin adjustment is shown. The pin is glued to the panel vertically and on precise positions that are given by alignment pins and holes on stiffbacks or templates produced by precise CNC milling machines. Before assembly all five panels must be leak tested using an appropriate test facility.

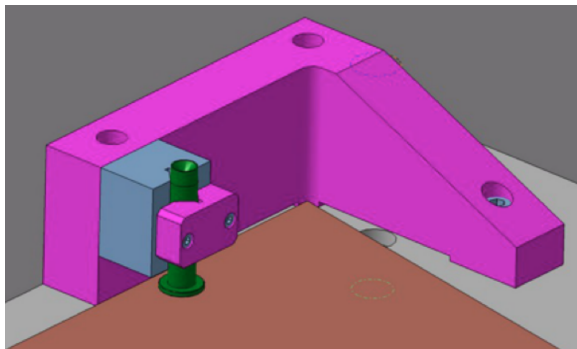


Fig. 15. The tool to position the precision pin on the lower readout panel with high accuracy and under 90.0° . The tool will be removed after glueing. The mounting position of the rigid clamps is given by precise pins in a stiffback or in a template.

To minimize the contamination of the assembled quadruplet with dust and dirt, the final assembly takes place in a clean room and in a vertical mounting structure as shown in fig. 16.

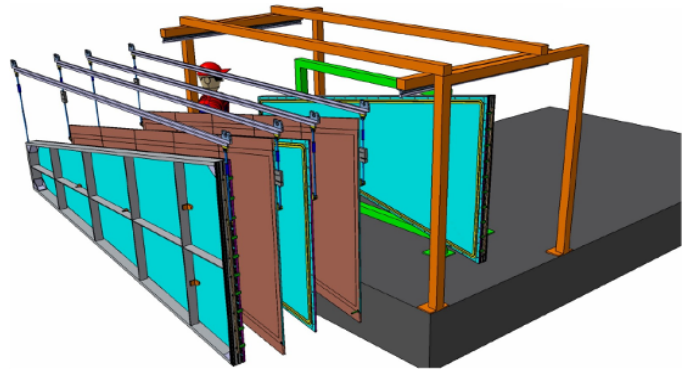


Fig. 16. Assembly of a quadruplet in a vertical mounting structure. The outer frames are reinforced by stiff frames which are removed after the assembly. Vertical mounting in a clean room reduces the influence of dust and dirt.

The panel assembly process starts with one of the outer drift panels mounted vertically to a solid holding frame. The outer drift panels are mounted additionally on stiffening frames since they experience a torque due to the stretched mesh which otherwise would cause bending of the panel.

The other panels are then guided by a linear bearing system that allows for precise adjustment of the precision pins or the precision washers in a force-free manner monitored by load cells. For the fine adjustment micrometer screws will be used.

Each time a drift and readout panel will be combined, a HV test will be performed. This is a very sensitive test to remaining dust particles that have to be removed before final assembly. After all panels are put together the quadruplet is fixed with screws. In a final step the external stiff frames are removed.

VII. FLATNESS OF SANDWICH PANELS

To meet the stringent mechanical requirements for individual panels, for the whole quadruplet and finally for the whole sector, the topology of the surfaces of a single panel is a figure of merit. Using either tactile or nontactile measurement methods, or both, the flatness of each panel has to be mapped. Fig. 17 shows the topology of one side of a sandwich panel of the mechanical prototype which was built using the two step glueing method.

It shows an almost perfect flatness inside the active area of the detector. Larger deviations are visible only at the borders of the panel. Reasons for these deviations have been investigated and result in stiffbacks with a 10-fold higher stiffness than the one used for this prototype.

Deviations from a planar surface are not only due to construction processes but can also result from operational conditions. Fig. 18 shows the assembly of four mechanical prototypes on a spacer frame placed on a large granite table. Deformations by intentionally induced temperature gradients could be measured and simulated. They were largely understood and lead to a modified holding structure of the modules in the final setup.

Since the detectors are filled with an overpressure of 2 mbar the whole quadruplet blows up during operation. To minimize the blow up interconnections are used which keep the thickness

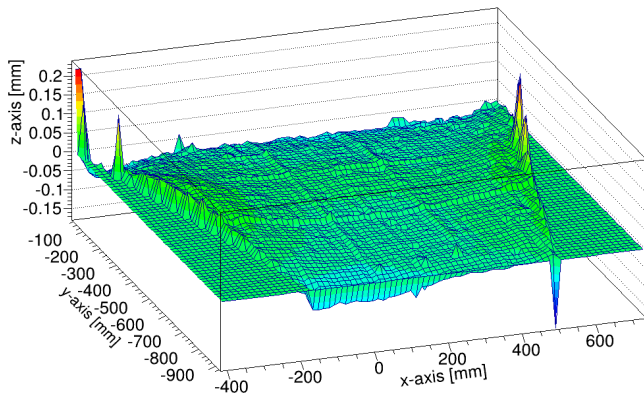


Fig. 17. Topology of a mechanical prototype panel obtained with a coordinate measurement machine. Deviations from the tolerances occur only at the border, outside the active area. The $15\ \mu\text{m}$ high grid like structure was intentionally provoked by grooves in the granite table. This allows easily for optical judgement of the planarity of the surface. The panels produced for the NSW will not show this grid like structure on their surfaces.

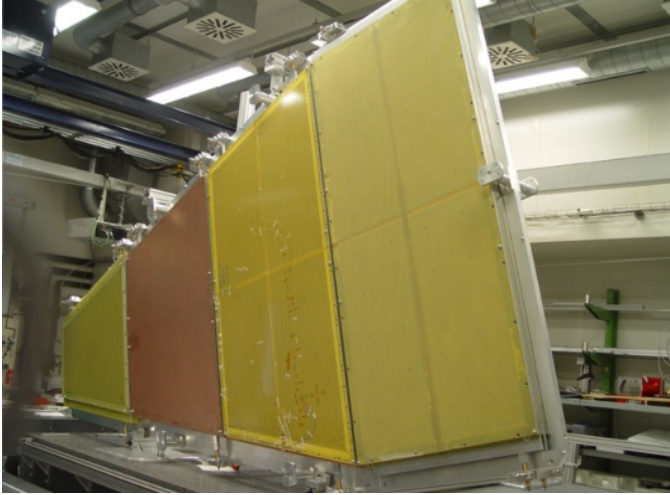


Fig. 18. For deformation and stability tests each of the four construction sites contributed a mechanical prototype built according to the structure of the final quadruplets. Only the active readout anodes were substituted by dummies and the segmentation of a sector was chosen to be four-fold. This picture shows a full size model of a large sector built by four modules mounted on the spacer frame in preparation for measurements as temperature dependence of surface planarity or reversibility of deformations provoked by temperature, stress or overpressure.

of the quadruplet constant. The layout of an interconnection is shown in fig. 19.

To find a minimal number and ideal positions of the interconnections simulations with the finite element code ANSYS [8] are investigated. Fig. 20 shows the result of a simulation with six interconnections in the SM2 module [9].

The maximum deformations are with $\approx 50\ \mu\text{m}$ well below the maximum tolerance.

VIII. CONCLUSION

We describe the feasibility, the design and construction of high-rate capable large size Micromegas chambers for the upgrade of the ATLAS muon spectrometer. To cope with the extreme requirements, as readout strip alignment within $30\ \mu\text{m}$ and surface planarities within $80\ \mu\text{m}$ precision, special

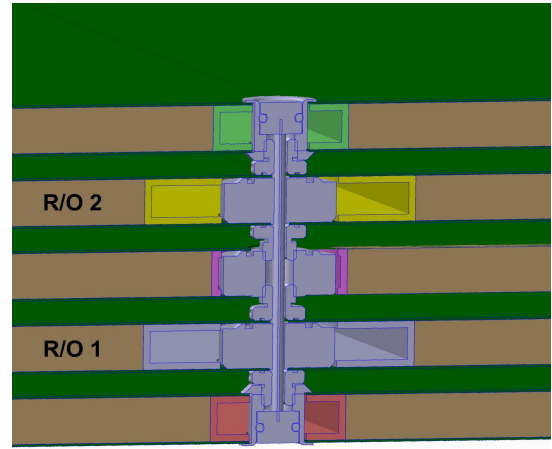


Fig. 19. An interconnection through the five sandwich panels. The almost planar areas directly around the interconnections on the top side of the quadruplet will be used for the precise positioning of alignment platforms for optical monitoring of thermal deformations of the quadruplets during active LHC runs.

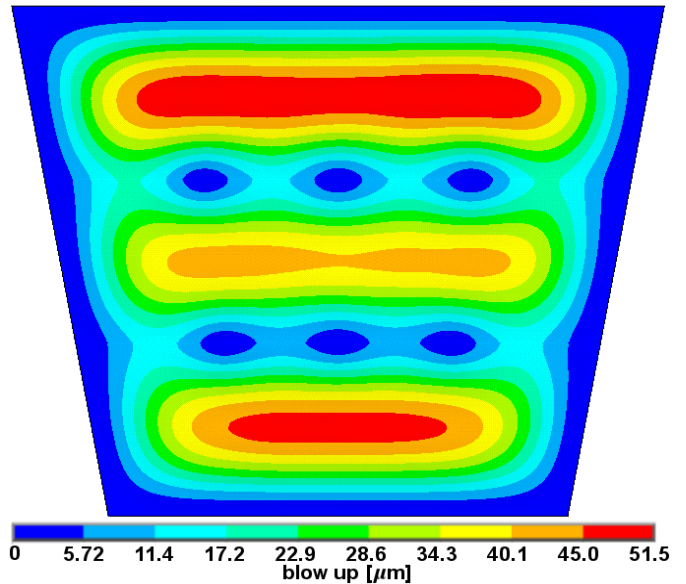


Fig. 20. Simulation of blow up of quadruplet due to $2\ \text{mbar}$ overpressure inside the chambers. This simulation shows the result using six interconnections. The maximum deviation is $\approx 50\ \mu\text{m}$.

methods and tooling had to be developed for these large detector modules having areas above $2\ \text{m}^2$. A basic idea is to transfer the planarity of precision surfaces, as granite tables, to the surface of the readout and drift panels. These panels consist of sandwich structures with surface sheets of three or five pieces of $0.5\ \text{mm}$ thick printed circuit boards and a core of aluminum honeycomb for stability. The drift panel PCBs form the cathodes and the readout panel PCBs the anodes of the detectors. The strip anodes are designed as resistive strips with specific resistivities around $10\ \text{M}\Omega$ per cm. The readout strips are coupled capacitively to the resistive strips and provide the signals for the front end electronics. Their strips are $300\ \mu\text{m}$ wide and have a pitch of 425 or $450\ \mu\text{m}$ for the small or large sectors, respectively. The width of the resistive strips is slightly smaller at identical pitch.

In this paper the working principle of resistive strip Micromegas detectors is explained. The design of the two New Small Wheels is separated into eight sectors. Each sector is subdivided into two trapezoidal subsectors. Each subsector consists of eight consecutive detector layers separated by a spacer frame into two quadruplets. The Micromegas quadruplets are built from five sandwich panels separated by precise extruded aluminum bars, the drift frames. This is presented in detail including the vertical assembly procedure. It is shown that the strict planarity requirements can be fulfilled. Methods are presented that allow for precise and exact alignment of the readout PCBs against each other. The stretching of meshes in the size needed for the NSW is possible. The cleaning of the meshes is still under investigation. Simulations have shown that the slight overpressure in the gas detectors leads to a deformation of the surface. To resolve this problem interconnection will be installed into the quadruplets, which keep the deformation to a minimum. Then the maximal deformation due to the overpressure will be only $50 \mu m$.

The construction principle allows for a series production of many large area micromegas detector modules while ensuring a $O(10 \mu m)$ level of mechanical accuracy for every module.

ACKNOWLEDGMENT

We acknowledge the support by the DFG Excellence Cluster Universe.

REFERENCES

- [1] ATLAS collaboration, *The ATLAS Experiment at the CERN Large Hadron Collider* JINST P08003 3 (2008)
- [2] Y. Giomataris et al., *MICROMEGAS: a high-granularity position-sensitive gaseous detector for high particle-flux environments* Nuclear Instruments and Methods in Physics Research Section A, Volume 376 (1996): 29 - 35
- [3] V. Smakhtin et al., *Thin Gap Chamber upgrade for SLHC: Position resolution in a test beam* Nuclear Instruments and Methods in Physics Research Section A, Volume 598 (2009): 196 - 200
- [4] ATLAS Collaboration, *Performance of the ATLAS Trigger System in 2010* The European Physical Journal C, Volume 72:1849 (2012)
- [5] ATLAS Collaboration, *ATLAS New Small Wheel Technical Design Report* ATLAS - TDR-20-2013 (2013) Available: <https://cds.cern.ch/record/1552862/files/ATLAS-TDR-020.pdf>
- [6] H. Raether, *Electron Avalanches and Breakdown in Gases* Butterworths (1964)
- [7] T. Alexopoulos et al., *A spark-resistant bulk-micromegas chamber for high-rate applications* Nuclear Instruments and Methods in Physics Research Section A, Volume 640 (2011): 110 - 118
- [8] ANSYS Inc., *ANSYS Mechanical APDL Element Reference* (2013) Available: <http://148.204.81.206/Ansys/150/ANSYS%20Mechanical%20APDL%20Element%20Reference.pdf>
- [9] E. Pree, *Construction of Large Size Micromegas Detectors* master thesis, LMU Munich (2014) Available: http://www.etp.physik.uni-muenchen.de/dokumente/thesis/master_epree.pdf